Laser Fusion Researches at ILE, Osaka

M. Murakami
Institute of Laser Engineering, Osaka University,

Abstract

Two different ignition approaches, fast ignition and impact ignition, under investigation at the institute of laser engineering, Osaka University, are reviewed. In the fast ignition, the result reported in Nature **412**, 798 (2001) has been reconfirmed to further aim at 5 keV heating with an invested laser energy of 10 kJ. In the impact ignition scheme, such distinctive milestones as a super-high velocity ~ 1000 km/s and an increase in neutron production by a factor of one hundred have been demonstrated experimentally.

1. Fast Ignition

After 50 years from the innovation of lasers, demonstration of controlled ignition and subsequent burn is expected within a couple of years at the US National Ignition Facility [1] (NIF). Fast ignition has the high potential to ignite a fuel using only about one tenth of laser energy of NIF. This compactness would extensively accelerate laser fusion energy development. One of the most advanced fast ignition programs is the Fast Ignition Realization Experiment [2] (FIREX). The goal of its first phase is to demonstrate ignition temperature of 5 keV, followed by the second phase to demonstrate the ignition-and-burn.

The initial experiment of FIREX-I was performed using deuterated polystyrene shells with a gold cone. Ion temperatures of the core plasmas were deduced from the observed neutron yield, fuel density and the fuel mass to be about 0.7 keV at the heating laser energy of 0.5 kJ, confirming the previous experimental result [3]. The coupling efficiency from the incident laser energy to the core plasma is estimated to be 15%, giving a confidence that ion temperature will increase up to the 5-keV level at the expected performance (10 kJ) of the heating laser.

It would take 10 years for technology development and 10 more years for power generation test. The technology includes high rep-rate lasers; target injection, tracking and beam staring; and fusion chamber and blanket. These technologies would be converged into an integrated engineering test facility, the goal of which is to repeatedly generate a core plasma of FIREX-I level at a 1-Hz rate. After the demonstration of repeated plasma production, a laser fusion experimental reactor would be started with the goal of demonstration of power generation around 2030. It is named Laboratory Inertial Fusion Test (LIFT). Below we describe a few different studies on high energy density physics going on at Institute of laser engineering.

2. Impact Ignition

In impact ignition scheme [4], a portion of the fuel (the impactor) is accelerated to a super-high velocity (Fig.1), compressed by convergence, and collided with a precompressed main fuel. This collision generates shock waves in both the impactor and the main fuel. Since the density of the impactor is generally much lower than that of the main fuel, the pressure balance ensures that the shock-heated temperature of the impactor is significantly higher than that of the main fuel. Hence, the impactor can reach ignition temperature and thus become an igniter.

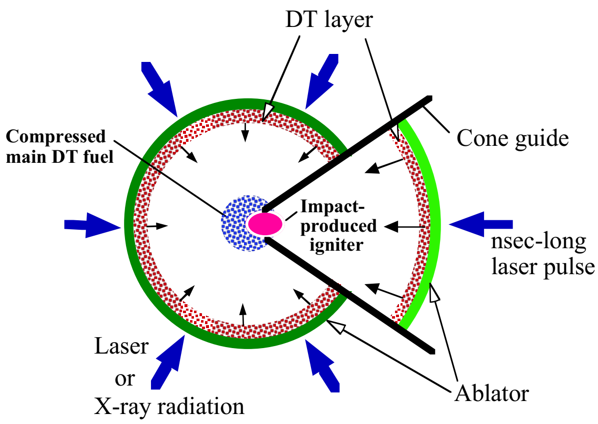

Fig.1 Both parts of the mpact ignition target (the main fuel and the impactor) are driven by ns-long pulses.

Here we report major new results on recent impact ignition research: (1) A maximum velocity ~ 1000 km/s has been achieved under the operation of NIKE KrF laser at Naval Research Laboratory (laser wavelength = 0.25μm) in the use of a planar target made of plastic and (2) We have performed two-dimensional simulation for burn and ignition to show the feasibility of the impact ignition.

2.1. Achievement of a Super-high Velocity ~ 1000 km/s

Impact ignition, as well as the other designs such as hot-electron-driven fast ignition and shock ignition, reduces driver energy requirement by heating a portion of DT fuel in terms of an additional heating mechanism. The significant advantage for these approach is to separate the compression from the heating. This report describes experiments that, for the first time, reach target velocities in the range of 700 – 1000 km/s. The highly accelerated planar foils of deuterated polystyrene, some with bromine doping, are made to collide with a witness foil to produce extreme shock pressures and result in heating of matter to thermonuclear temperatures. Target acceleration and collision are diagnosed using large field of view monochromatic x-ray imaging with backlighting as well as bremsstrahlung self-emission. The impact conditions are diagnosed using DD fusion neutron yield, with over 10^6 neutrons produced during the collision. Time-of-flight neutron detectors are used to measure the ion temperature upon impact, which reaches 2 – 3 keV. The experiments are performed on the Nike facility, reconfigured specifically for high intensity operation. The short wavelength and high illumination uniformity of Nike KrF laser uniquely enable access to this new parameter regime. Intensities of (0.4 − 1.2) x 10^{15} W/cm^2 and pulse durations of 0.4 − 2 ns were utilized in the experiments. As a result of a series of experiments using NILE laser at Naval Research Laboratory, a super-high velocity of a laser-driven foil of about 1000 km/s has been achieved [5]. Figures 2 and 3 show the experimental set-up and the x-ray image of the foil acceleration.

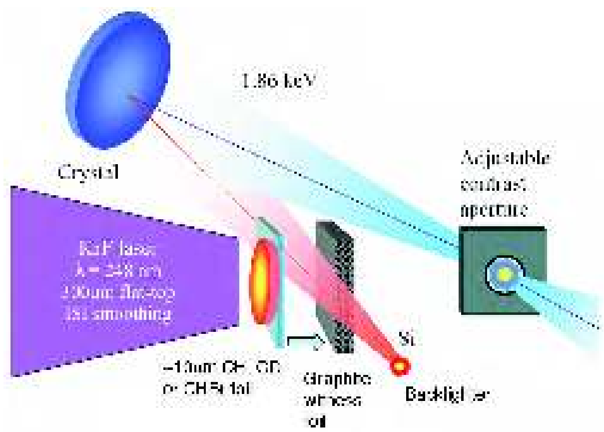

Fig.2 Experimental set up

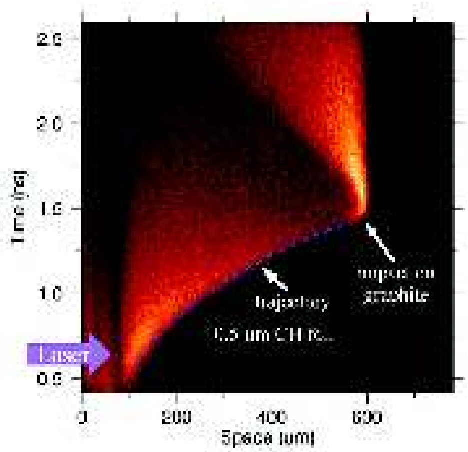

Fig.3 X-ray image

2.2. Two-dimensional simulation for ignition and burn

Modeling of the target acceleration, collision, and neutron production is preformed using the two-dimensional radiation hydrodynamics code with a non-LTE radiation model. Moreover, detailed analytical model addresses the feasibility of even higher velocities.Our hydrodynamic simulation shown in Fig. 4 demonstrates [6] that ignition occurs when an impactor with a velocity of 1750 km/s and a density of 50 g/cm^3 collides with the main fuel with a density of 400 g/cm^3. Here, the implosion and acceleration processes are neglected. The impactor in a bullet-shape initially has spatial extensions of 60 and 70 μm in the perpendicular and the parallel directions with respect to the collision axis, respectively. The main fuel has a concave shape to tamp the impactor, as is observed in an implosion with a cone. The impactor energy is only about E_i ~ 10 kJ, whereas the main fuel has a much higher energy than this. However, if the energy of the main fuel is reduced so that it is one to two times the impactor energy, i.e., E_m ~ 10-20 kJ, and if a typical coupling efficiency of η_c ~ 10 % from the laser to the internal energy of the fuel assembly is assumed, we estimate that the laser energy for ignition will be $E_L = (E_i+E_m)/\eta_c$ ~ 200-300 kJ. This energy is much lower than that required for central hot spot ignition and is comparable to that required for conventional fast ignition. The primary challenges are thus to generate such high velocities while maintaining target integrity and to achieve such high impactor densities. Throughout this study, unless stated otherwise, we define the time origin as the time of maximum compression of the main fuel.

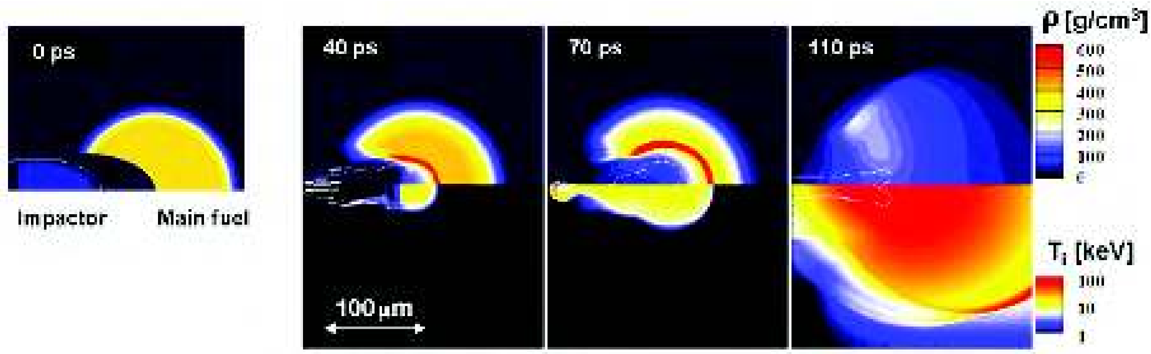

Fig. 4 Snapshots of density and temperature distributions obtained from the two-dimensional simulation. At t = 110 ps, ignition and burn can be observed with temperatures > 30 keV.

2. Optimization of laser illumination configuration

A crucial requirement to achieve laser fusion is to illuminate a fusion pellet as uniformly as possible with a limited number of laser beams. Presently, there are only a few big lasers in current operation based on direct-drive, the counter scheme to the indirect-drive, that directly illuminates a spherical pellet. Although direct drive is expected to achieve a higher energy coupling than the indirect-drive scheme, high irradiation uniformity is more difficult to achieve. So far some work on the irradiation system have been reported on the direct-drive scheme, which are in principle based on geometrical considerations. Here we propose a new numerical algorithm to give an optimum direct-drive beam configuration for highly uniform irradiation [7]. It is obtained as a self-organizing system by solving an N-body charged particle simulation and is applicable for an arbitrary number of beams.

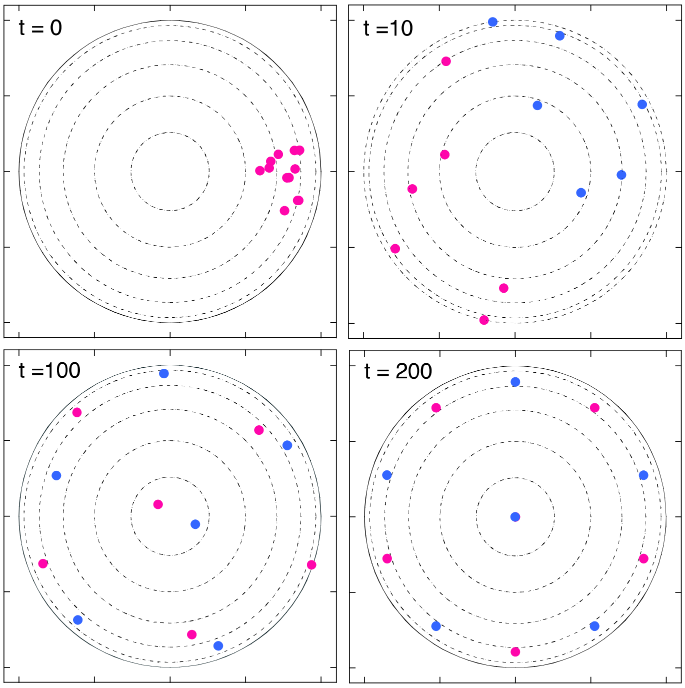

Fig.5 Temporal evolution of the positions of twelve charged particles on a sphere at different time steps. The points are projected on the xy- (or equatorial-) plane normal to the view axis (z-axis), where the blue and red colors denote that they are on the north and south hemisphere, respectively. The final configuration at t = 200 coincides with that of the dodecahedron.

3.1. Self-organizing electro-dynamic system

Suppose that N_B charged particles are initially randomly distributed on a sphere and are redistributed due to the Coulomb repulsion to settle at a fixed configuration in a self-organized manner. Our hypothesis is then as follows: If one finds such a configuration of N_B charged particles on a sphere that has the lowest Coulomb potential energy, the resulting system gives the highest irradiation uniformity. The radial beam axes are determined from the particle positions thus obtained. The present method reproduces Platonic solids with $N_B = 4$, 6, and 12 except for $N_B = 8$ and 20. Moreover, new configurations, such as M48 and M72, have been found that demonstrate even better performance in achieving higher irradiation uniformity than the other configurations, where the notation "M48", for example, stands for the solution obtained by the present method with $N_B = 48$. In addition, we use the notation

"P12" (dodecahedron), "P20" (icosahedron), and "P32" (12 faces and 20 vertices of dodecahedron) for Platonic solids and their secondary solids. In fact, according to numerical surveys (details of the comparisons are not presented in this paper), the latter (spherical) shows higher performance as an illumination system than the former (cylindrical). At $t = 0$, N_B charged particles are randomly distributed on the sphere, and they move around on the sphere.

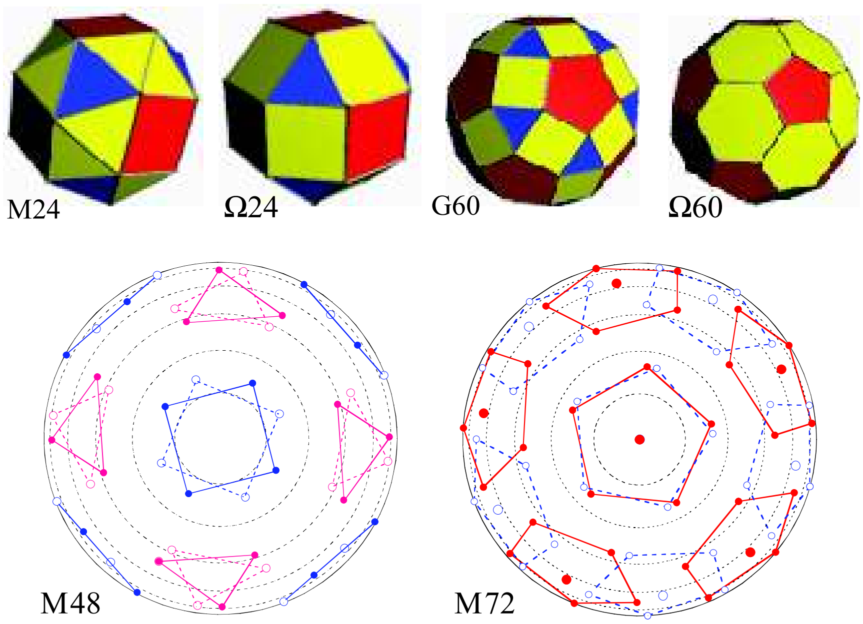

Fig.6 Perspective views of some irradiation configurations; M24, M48, and M72 are obtained by the present N-body simulation, Ω24 and Ω60 are ones of the actual laser systems at LLE, Rochester Univ., and G60 for $N_B = 60$ was proposed by Murakami (1995) based on geometrical considerations. Laser beams are expected to irradiate the target with their beam axes through the vertices. The solid and dotted circles of M48 and M72 denote that they are on the opposite hemispheres to each other.

Figure 5 shows the temporal evolution of the positions of twelve charged particles on a sphere at time steps, t = 0, 10, 100, and 200, obtained from a simulation for M12. At t = 0, the twelve particles are put on the sphere clustered close to each other. The particles on the sphere are projected on the xy- (or equatorial-) plane normal to the view axis (z-axis), where the blue and red colors denote that they are on the north and south hemisphere, respectively. The concentric dashed curves stand for the projections of equi-latitude circles of 15°, 30°, 45°, 60°, and 75° measured from the pole axis. In the final configuration at t = 200, the twelve particles settle down at the face centers of the dodecahedron, as expected. Thereby ten particles, all except for the two at the poles, have polar angle $\theta = 63.43°$ or 116.6°, being positioned symmetrically on the same equi-latitude circles.

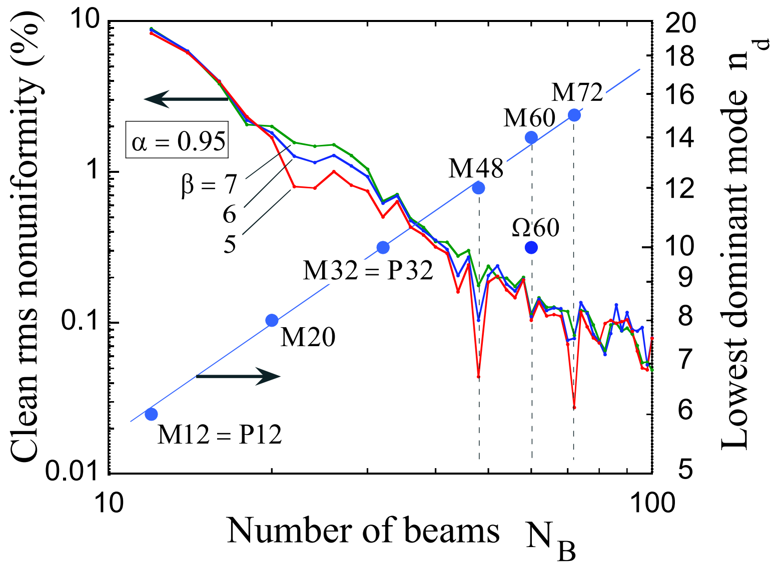

Fig.7 Lowest dominant mode number n_d (blue circles) and the clean rms nonuniformity σ^0_{rms} versus the number of beams N_B. The blue straight line stands for an analytical prediction obtained from geometrical considerations.

Figure 6 shows perspective views of some irradiation configurations: M24, M48, and M72 are obtained by the present method, while Ω24 and Ω60 are ones used by the laser systems at LLE, Rochester Univ., and G60 for N_B = 60 was proposed in Ref. [8] based on geometrical considerations. The solid and open circles for M48 and M72 denote that they are assigned to different hemispheres. Laser beams are expected to irradiate the target with their beam axes through the vertices. The four 3-dimensional (3d) views shown in Fig. 6 for M24, G60, Ω24 and Ω60 show only the topological structures of the corresponding solids of the 13 Archimedean solids, rhombicosidodecahedron, and truncated icosahedron, respectively; the optimum beam positions obtained by the present method are slightly different than those 3d views. Concerning the three 60-beam designs, i.e., M60, G60, and Ω60, roughly speaking, better performance with high flexibility to many different beam patterns are found in the systems just in this order. Careful observation reveals that M24, M48 and M72 have very geometrically symmetric patterns. For example, in M48, equilateral triangles and squares are regularly allocated on the faces of a truncated octahedron. In the case of M72, twelve regular pentagons, each of which are composed of 6 points including the central points, are allocated on the dodecahedron faces, as can be seen in Fig. 6. It should be noted that most of the obtained patterns with different numbers of N_B are twisted along z-axis in a left-(or right-

)handed-screw manner. In other words, there always exists another solution with the opposite twist at the same lowest potential energy E_p. Moreover, most of the optimized patterns obtained by the present method have no pair of points that are antipodes of each other (the twelve face centers of dodecahedron in M72 are rather exceptional). This is a pronounced advantage in view of optical system protection. Additionally, the present algorithm can give a best irradiation configuration not only for even numbers but also for odd numbers of N_B.

Figure 7 plots the lowest dominant mode n_d and the clean rms nonuniformity σ_{rms}^0 versus N_B, that are numerically obtained using the present method, to show how the irradiation uniformity is improved by increasing N_B. The good reproducibility indicates that our hypothesis (that is, the charge distribution with a smallest E_p brings about the best laser fusion configuration) seems to hold.

3. Conclusion

By extending the demonstrated velocity from 640 km/s to over 1500 km/s, the energy efficiency from 2% to 10%, and taking the convergence effect into account, we estimate the laser energy necessary to create a hot spark to ignite DT fusion fuel to be 200–300 kJ. Of course, we are still uncertain how the above extension can be made. Presumably this extension might require appreciably shorter wavelength lasers than were used in this study, such as KrF lasers or fourth harmonics of Nd:glass lasers. Scaling up from the present experiments demonstrates that full-scale impact ignition could be attained within a practically allowable range.

References

[1] MOSES, E.I., Nucl. Fusion **49** (2009) 104022.

[2] AZECHI, H. *et al*., Nucl. Fusion **49** (2009) 104024.

[3] KODAMA, R. *et al*., Nature **418** (2002) 933.

[4] MURAKAMI, M. *et al*., Nucl. Inst. & Meth. Phys. Res. A**544** (2005) 67.

[5] KARASIK, M. *et al*., Phys. Plasmas **17**, (2010) 056317.

[6] AZECHI, H., *et al*., Phys. Rev. Lett. **102** (2009) 235002.

[7] MURAKAMI, M. et al., Phys. Plasmas **17**, (2010) 082702

[8] MURAKAMI, M., Appl. Phys. Lett. **66** , (1995) 1587.